

The microwave spectrum and structure of the methanol·SO₂ complex

Linghong Sun, Xue-Qing Tan, Jung Jin Oh, and Robert L. Kuczkowski
Department of Chemistry, University of Michigan, Ann Arbor, Michigan 48109

(Received 8 May 1995; accepted 18 July 1995)

The rotational spectra of nine isotopomers of the methanol-sulfur dioxide van der Waals complex were observed with a pulsed molecular beam Fourier transform microwave spectrometer. Each rotational transition is split into an *A*-state ($m=0$) and an *E*-state ($m=\pm 1$) transition due to methyl top internal rotation effects. The *A* and *E* transitions show an additional inversion splitting ranging from a MHz to a few tens of MHz in seven of the isotopomers. The inversion splitting is absent in the two S¹⁶O¹⁸O isotopomers. The center frequencies of the inversion doublets were used in a simultaneous fit of both the *A*- and *E*-state transitions, producing rotational constants which allowed a complete determination of the structure of the complex. Analysis of the moments of inertia indicate that the complex has a stacked structure. The center of mass distance between the two monomers is 3.08(5) Å. The effective torsional barrier height is $V_3=128.6(1)$ cm⁻¹ based on the assumption that the methyl group rotates against a heavy frame. The dipole moment is $\mu_T=1.94(3)$ D. The inversion motion is discussed based on effects on the splitting associated with isotopic substitution and the transition dipole direction. © 1995 American Institute of Physics.

I. INTRODUCTION

With recent advances in high-resolution spectroscopic techniques, there has been a growing number of investigations of weakly bound complexes. It is expected that the study of a group of related complexes will be helpful in determining trends in the configuration and properties of complexes, which in turn will lead to a better understanding of intermolecular forces. Several complexes containing SO₂ and an amine Lewis base, such as trimethylamine (TMA)·SO₂ (Ref. 1) and dimethylamine (DMA)·SO₂ (Ref. 2), have been studied. In these complexes the interaction between the sulfur atom and the nitrogen atom lone-pair electrons appears to be the dominate force which binds the monomers and it occurs with appreciable polarization effects. These are relatively strong complexes with nitrogen-to-sulfur interaction distances [$d(N-S)\approx 2.3$ Å] which are considerably smaller than the sum of the van der Waals radii of sulfur and nitrogen. Recently, the study of SO₂ containing complexes was extended to the R₂O·SO₂ system, where N is replaced with O and R is either a hydrogen or a methyl group. In water·SO₂ (Ref. 3) and dimethyl ether·SO₂ (Ref. 4) the complexes are stacked and the dipole moments of the two monomers are aligned nearly antiparallel in the complexes. This apparent dipole-dipole interaction supplements the polarizing interaction of sulfur with the oxygen lone-pair electrons which is of lesser importance based on the much larger distance between sulfur and oxygen (~2.9 Å). Another interaction that can play a role in SO₂ complexes involves methyl groups. In the methylacetylene·SO₂ complex,⁵ one of the oxygen atoms in SO₂ appears to be attracted to a methyl hydrogen, as evidenced by an eclipsed arrangement of the C-CH₃ bond and a S-O bond. Obviously, this interaction will enhance the binding strength of the complex. There are indications that this kind of interaction also influences the large amplitude internal vibrations and tunneling motions in the complex.

In view of this interplay of interaction effects, it seemed

worthwhile to extend the investigation of the R₂O·SO₂ series to the methanol·SO₂ complex. To our knowledge there has been no previous spectroscopic study of this complex. Methanol has a significant dipole moment of 1.69 D, which should give rise to a strong dipole-dipole interaction with SO₂. Both the hydroxyl hydrogen and methyl group in methanol can interact with the oxygen atoms in SO₂. It was of interest to explore the effect of the relative competition of these interactions on the structure. It was also of interest to determine the barrier to internal rotation of the methyl group since a decrease in this barrier height has been observed in the CH₃OH·NH₂CHO (Ref. 6), CH₃OH·CO (Ref. 7), and CH₃OH·Ar (Ref. 8) complexes. It was recently proposed⁹ that this lowering in the torsional barrier height is an artifact arising from neglect of the large amplitude vibrational motion of the methanol subunit within the complex.

II. EXPERIMENT

The methanol·SO₂ complex was generated in a supersonic expansion of a gas mixture of roughly 2% methanol and 2% SO₂ seeded in 96% of Ne-He carrier gas (80% Ne and 20% He). The backing pressure was about 2 atm. The spectrum intensity decreased by about fifty percent when Ar was used as the carrier gas. Spectrophotometric grade methanol (Mallinckrodt) was used in the experiment. CH₃OD (99% D), CD₃OH (99.5% D), ¹³CH₃OH (99% ¹³C), and CH₃¹⁸OH (94% ¹⁸O) were purchased from Isotec. CD₃OD (99.5% D) was obtained from Aldrich. S¹⁸O₂ (97% ¹⁸O) was purchased from Icon. The S¹⁶O¹⁸O species was made by mixing equal amounts of S¹⁶O₂ and S¹⁸O₂ in a sample bulb. They exchange quickly and give a ratio of 2:1:1 for S¹⁶O¹⁸O:S¹⁶O₂:S¹⁸O₂.

The rotational transitions of methanol·SO₂ were observed using a Balle-Flygare type Fourier transform microwave spectrometer.¹⁰ The spectrometer operated between 7.3–18 GHz. Spectral linewidths were typically 30–50 kHz full width at half maximum resulting from Doppler broaden-

ing. Usually the measured line frequencies were reproducible to within ± 5 kHz.

Stark effect measurements were used to determine the J quantum number of the transitions and the dipole moment components of the complex. Moreover, Stark effect measurements were helpful in determining whether a particular rotational transition was associated with the $A(m=0)$ or the $E(m=\pm 1)$ torsional states. The spectrometer was equipped with two parallel steel mesh plates 30 cm apart straddling the microwave cavity.¹¹ A dc voltage up to 9.9 kV was applied with opposite polarity to each plate. The $J=1 \leftarrow J=0$ transition of OCS ($\mu = 0.715\ 196$ D) (Ref. 12) was used to calibrate the electric field at each voltage.

III. RESULTS AND ANALYSIS

The methanol·SO₂ spectrum exhibited all three dipole selection rules. The a -type transitions were the most intense. Most of the transitions appeared either as doublets or quartets. The splitting varied from about one MHz to a few tens of MHz within a doublet or quartet. This splitting was initially thought to arise from internal rotation of the methyl group, leading to a preliminary estimate¹³ of the torsional barrier which was too high. We subsequently realized that this splitting arose from some kind of inversion motion. This is discussed more fully in Sec. IV B 1. The proper assignment of the doublets was accomplished with the aid of Stark effect measurements. The transitions showing a second-order Stark effect were associated with the A torsional state; the transitions showing a first-order Stark effect were associated with the E torsional state (except for $K_a=0$ transitions). A total of 22 pairs (with $K_a \leq 2$) of A -state transitions were observed. The A -state transition pairs exhibited an inversion splitting of different magnitude depending on the dipole type. The inversion splitting was approximately 1 MHz for the a -type transitions, 30 MHz for the b -type transitions, and 6 MHz for the c -type transitions. A total of 20 sets (with $K_a \leq 2$) of E -state transitions were observed. The E -state transitions showed an inversion splitting of similar magnitude as that observed for the A -state transitions. Unlike the A -state transitions, the E -state transitions should, in principle, appear as quartets due to a mixing of the rotational basis functions of different symmetries.⁵ The quartets consist of two pairs of transitions, grouped as an inner pair and an outer pair. Sometimes one of the pairs was not observed because of low intensity, resulting in a doublet. The observed A and E state transitions are listed in Tables I and II.

A complete (PAM) torsion-rotation Hamiltonian typically used in methyl group internal rotation problems^{14,15,16} was first used to fit the average frequency (ν_{ave}) of the transition doublets (or quartets) for the A and E states. The standard deviation for the fit was several hundred kHz. With the addition of an extra linear term, $D_a P_a$, the standard deviation was reduced to about 20 kHz. This modified Hamiltonian is given as

TABLE I. Observed microwave transitions (MHz) of methanol·SO₂ (normal species, A lines).

J'	K'_a	K'_c	J''	K''_a	K''_c	ν_{obs}^a	ν_{ave}^b	Obs.—Cal. ^c
3	0	3	2	1	2	7844.668(-,+) 7877.979(+,-)	7861.323	0.016
2	1	2	1	1	1	7929.003(+,+) 7930.241(-,-)	7929.622	0.055
2	0	2	1	0	1	8262.570(+,+) 8263.637(-,-)	8263.103	0.003
2	1	1	1	1	0	8633.614(+,+) 8633.865(-,-)	8633.739	-0.039
1	1	1	0	0	0	8942.291(+,+) 8980.104(+,-)	8961.197	-0.068
1	1	0	0	0	0	9310.811(+,+) 9316.561(-,-)	9313.686	0.066
3	1	3	2	1	2	11 881.696(+,+) 11 883.516(-,-)	11 882.606	0.018
3	0	3	2	0	2	12 347.268(+,+) 12 348.951(-,-)	12 348.110	-0.001
4	0	4	3	1	3	12 343.387(-,+) 12 372.521(+,-)	12 357.954	-0.009
3	2	2	2	2	1	12 425.677(+,+) 12 426.120(-,-)	12 425.898	-0.003
3	2	1	2	2	0	12 491.807(-,-) 12 492.487(+,+)	12 492.147	0.003
2	1	2	1	0	1	12 731.860(-,+) 12 767.921(+,-)	12 749.890	0.015
3	1	2	2	1	1	12 938.166(+,+) 12 938.554(-,-)	12 938.360	-0.012
2	1	1	1	0	1	13 803.753(+,+) 13 809.231(-,-)	13 806.492	0.021
2	2	0	2	1	1	14 476.867(-,+) 14 492.909(+,-)	14 484.888	0.006
2	2	1	2	1	2	15 504.528(-,+) 15 520.217(+,-)	15 512.373	0.009
4	1	4	3	1	3	15 821.314(+,+) 15 823.634(-,-)	15 822.474	0.008
3	1	3	2	0	2	16 352.810(-,+) 16 385.981(+,-)	16 369.396	0.003
4	0	4	3	0	3	16 378.057(+,+) 16 380.415(-,-)	16 379.236	-0.008
4	2	3	3	2	2	16 548.209(+,+) 16 548.359(-,-)	16 548.284	-0.008
4	2	2	3	2	1	16 729.322(-,-) 16 729.716(+,+)	16 729.519	0.007
4	1	3	3	1	2	17 226.941(+,+) 17 227.474(-,-)	17 227.208	-0.008

^aObserved transition frequencies. Also given (in parentheses) are the inversion state assignments, (p', p''). When $p = '+'$ the specified state is associated with the inversion state of positive parity (or symmetric species in group theoretical language). When $p = '-'$ the specified state is associated with the inversion state of negative parity (or antisymmetric species).

^bThe average experimental frequencies of the inversion doublets.

^cThe differences between the averaged experimental frequencies (for the inversion doublets) and the corresponding calculated transition frequencies.

$$\begin{aligned} \mathcal{H} = & AP_a^2 + BP_b^2 + CP_c^2 + D_a P_a + \mathcal{H}_d^{(1)} \\ & + \frac{1}{2} \sum_{i \neq j}^{a,b,c} D_{ij} (P_i P_j + P_j P_i) - 2 \sum_i^{a,b,c} Q_i P_i P + F P^2 \\ & + V_3 (1 - \cos 3\alpha) / 2 + \mathcal{H}_d^{(2)}, \end{aligned} \quad (1)$$

where

TABLE II. Observed microwave transitions (MHz) of methanol·SO₂ (normal species, *E* lines).

<i>J'</i>	<i>K'_a</i>	<i>K'_c</i>	<i>J''</i>	<i>K''_a</i>	<i>K''_c</i>	ν_{obs} (inner pair)	ν_{obs} (outer pair)	ν_{ave}	Obs. - Cal.
3	0	3	2	1	2	8050.286	8068.322	8050.699	0.008
						8051.110	8033.075		
2	1	2	1	1	1	8103.237		8104.742	-0.006
						8016.248			
2	0	2	1	0	1	8233.313		8233.778	-0.001
						8234.243			
2	1	1	1	1	0	8463.969		8465.428	0.002
						8466.886			
1	1	1	0	0	0	8511.366	8491.140	8511.658	-0.003
						8511.949	8532.175		
1	1	0	0	0	0	9716.978		9717.374	0.002
						9717.770			
3	1	3	2	1	2	11 992.427		11 994.183	0.008
						11 995.936			
3	0	3	2	0	2	12 307.524		12 308.210	-0.001
						12 308.897			
4	0	4	3	1	3		12 371.061	12 386.053	-0.003
							12 401.044		
3	2	1	2	2	0	12 452.354		12 453.148	0.001
						12 453.943			
3	2	2	2	2	1	12 456.995		12 457.554	-0.009
						12 458.114			
2	1	2	1	0	1		12 472.515	12 491.290	-0.009
							12 510.065		
3	1	2	2	1	1	12 831.752		12 832.960	-0.009
						12 834.167			
2	1	1	1	0	1	14 056.074		14 057.692	0.004
						14 059.309			
4	1	4	3	1	3	15 891.014		15 892.466	-0.003
						15 893.918			
3	1	3	2	0	2		16 235.144	16 251.699	0.005
							16 268.254		
4	0	4	3	0	3	16 328.663		16 329.540	0.000
						16 330.416			
4	2	3	3	2	2	16 632.292		16 633.052	0.004
						16 633.811			
4	2	2	3	2	1	16 634.475		16 635.531	-0.005
						16 636.587			
4	1	3	3	1	2	17 161.320		17 161.865	0.010
						17 162.410			

$$A = A_r + F\rho_a^2, \quad B = B_r + F\rho_b^2, \quad C = C_r + F\rho_c^2,$$

$$D_{ij} = F\rho_i\rho_j \quad (i, j = a, b, c, \quad i \neq j),$$

$$Q_i = F\rho_i \quad (i = a, b, c),$$

$$F = F_0 \left(1 - \sum_i^{a,b,c} \rho_i \lambda_i \right)^{-1},$$

$$\rho_a = \frac{A_r}{F_0} \lambda_a, \quad \rho_b = \frac{B_r}{F_0} \lambda_b, \quad \rho_c = \frac{C_r}{F_0} \lambda_c.$$

Note that $D_a P_a$ was added as a phenomenological term and its interpretation was unclear. It will be shown later that it is likely related to the inversion motion. $A_r (= \hbar^2/2I_a)$, $B_r (= \hbar^2/2I_b)$, and $C_r (= \hbar^2/2I_c)$ are the rotational constants of the complex. $F_0 (= \hbar^2/2I_a)$ is the rotational constant of the methyl top about its C_3 symmetry axis. λ_a , λ_b , and λ_c are the direction cosines of the methyl group symmetry axis with respect to the principal axes of the complex.

$\mathcal{H}_d^{(1)}$ contains the distortion terms in the usual Watson A -reduction Hamiltonian. $\mathcal{H}_d^{(2)}$ is the torsional state-dependent distortion Hamiltonian,^{15,16}

$$\begin{aligned} \mathcal{H}_d^{(2)} = & -D_{Jm} P^2 p^2 - D_{Km} P_a^2 p^2 - D_{K3m} P_a^3 p \\ & -d_{Km} [P_a(P_b^2 - P_c^2) + (P_b^2 - P_c^2)P_a] p \\ & + d_m p^2 (P_+^2 + P_-^2) + 2L_{Ja} P^2 P_a p + 2L_{Jb} P^2 P_b p \\ & + 2L_{Jc} P^2 P_c p + H_{JKm} P^2 P_a p^2. \end{aligned} \quad (2)$$

Note that a sextic term was added to improve the fits. Implementation of Eqs. (1) and (2) has been discussed before.⁵ The rotational temperature used in the simulations was 1.2 K. A simultaneous fit of all the observed A lines and E lines was carried out. The fitted molecular constants are reported in Table III. Note that not all the distortion terms in Eq. (2) were used. The unused ones were set at zero. The deviation for the fit, $\Delta\nu_{\text{rms}} = 19$ kHz (see Table III), is about 4

TABLE III. Molecular constants of CH₃OH·SO₂ and its isotopomers (uncertainties represent one standard deviation in the least-squares fit).

	CH ₃ OH·SO ₂	CH ₃ ¹⁸ O·SO ₂	¹³ CH ₃ OH·SO ₂	CH ₃ OD·SO ₂	CD ₃ OH·SO ₂	CD ₃ OD·SO ₂	CH ₃ OH·S ¹⁸ O ₂	CH ₃ OH·S ¹⁶ O ¹⁸ O	CH ₃ OH·S ¹⁸ O ¹⁶ O
<i>A_r</i> (MHz)	7074.838(62)	6974.147(61)	7055.488(65)	6853.126(127)	6697.738(246)	6487.542(674)	6505.318(65)	6829.462(65)	6747.624(26)
<i>B_r</i> (MHz)	2233.903(14)	2180.547(9)	2176.255(16)	2216.086(26)	2033.970(26)	2024.780(62)	2185.922(12)	2193.893(13)	2224.129(11)
<i>C_r</i> (MHz)	1884.065(23)	1842.699(9)	1842.871(18)	1856.621(24)	1742.979(25)	1721.743(59)	1816.270(23)	1845.242(24)	1853.848(20)
<i>Δ_J</i> (kHz)	5.90(22)	5.97(7)	5.25(11)	6.93(6)	6.60(4)	6.32(6)	5.59(22)	5.67(22)	5.68(20)
<i>Δ_{JK}</i> (kHz)	12.33(44)	11.65(46)	11.13(48)	7.80(49)	7.10(116)	4.69(36)	9.99(30)	8.17(27)	13.46(26)
<i>δ_J</i> (kHz)	0.49(9)	0.60(4)	0.25(1)	0.64(3)	0.67(4)	0.68(5)	0.30(9)	0.41(9)	0.32(9)
<i>δ_K</i> (kHz)	-22.05(319)	-15.44(389)	-25.26(414)	29.38(289)	0.0 ^a	19.48(311)	0.0	0.0	0.0
<i>D_a</i> (MHz) ^b	5.594(4)	5.194(7)	5.134(8)	0.0	3.079(7)	0.0	4.615(7)	0.0	0.0
<i>Δ_{inv}</i> (MHz) ^c	22.04(3)	20.46(3)	20.25(3)	1.49(2)	12.21(2)	0.68(1)	18.54(2)	0.0	0.0
<i>V₃</i> (cm ⁻¹)	128.665(4)	129.530(3)	128.726(3)	164.795(10)	107.186(10)	139.112(2)	128.649(4)	128.964(4)	128.596(3)
<i>F</i> (cm ⁻¹)	5.3	5.3	5.3	5.3	2.65	2.65	5.3	5.3	5.3
<i>λ_a</i>	0.571(5)	0.558(4)	0.575(4)	0.552(10)	0.611(19)	0.599(25)	0.571(5)	0.576(5)	0.557(4)
<i>λ_b</i> ^d	0.703	0.715	0.701	0.715	0.689	0.690	0.693	0.684	0.716
<i>λ_c</i>	0.424(12)	0.421(8)	0.421(10)	0.430(26)	0.389(52)	0.407(68)	0.440(10)	0.447(11)	0.420(9)
<i>D_{Jm}</i> (MHz)	-3.664(3)	-3.413(2)	-3.672(2)	-3.084(3)	-2.583(6)	-2.061(13)	-3.585(3)	-3.710(3)	-3.605(3)
<i>D_{Km}</i> (MHz)	12.810(22)	12.568(22)	13.074(24)	11.469(39)	4.171(65)	4.951(13)	11.977(23)	13.887(23)	12.752(8)
<i>L_{Ja}</i> (MHz)	0.068(30)	0.081(3)	0.055(3)	0.062(5)	0.032(11)	0.0	0.023(3)	0.054(3)	0.077(3)
<i>L_{Jb}</i> (MHz)	-0.049(21)	0.0	-0.092(9)	0.0	0.0	0.0	-0.086(23)	-0.100(23)	-0.080(20)
<i>n</i> ^e	42	41	40	38	37	30	38	41	47
<i>Δν_{rms}</i> (kHz) ^f	19	20	21	9	16	14	17	17	13

^aParameters not listed in this table were set equal to zero.^b*D_a* is the coefficient of the linear term in Eq. (1).^c*Δ_{inv}* is the pure inversion splitting.^d*λ_b* was adjusted in the fits according to $\lambda_a^2 + \lambda_b^2 + \lambda_c^2 = 1$.^eNumber of observed transitions in the fit.^f $\Delta\nu = \nu_{\text{obs}} - \nu_{\text{calc}}$.

TABLE IV. Stark coefficients for the ground torsional state ($m=0$) transitions and dipole moment of methanol·SO₂.

Transition	$ M $	$\Delta\nu/\epsilon^{2,a}$	Obs-Calc.
$3_{03}-2_{02}$	0	-0.059	0.000
	1	-0.006	0.000
	2	0.153	0.002
$2_{02}-1_{01}$	0	-0.257	0.000
	1	0.317	-0.001
$3_{13}-2_{12}$	0	-0.021	-0.002
	1	0.189	0.003
	2	0.801	-0.001
$4_{04}-3_{03}$	0	-0.021	0.001
	1	-0.010	0.000
	2	0.028	-0.001
	3	0.091	-0.001

$$\begin{aligned} |\mu_a| &= 1.781(2) \text{ D}^b \\ |\mu_b| &= 0.543(23) \text{ D} \\ |\mu_c| &= 0.554(22) \text{ D} \\ |\mu_T| &= 1.94(3) \text{ D} \end{aligned}$$

^aObserved Stark coefficients in units of 10^{-4} MHz/(V/cm)².

^bThe uncertainties are 1σ .

times that of the experimental uncertainty. This apparently is caused by the inadequacy of the Hamiltonian used in the fit. But the molecular constants obtained from the fit should be good enough to allow structural and dynamical information to be extracted.

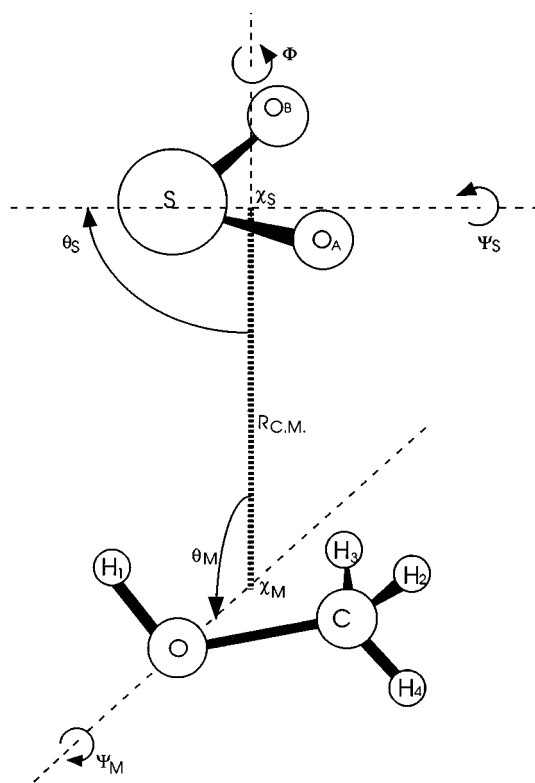
The spectra of the following isotopic species have also been observed: ¹³CH₃OH·SO₂, CH₃¹⁸OH·SO₂, CH₃OH·S¹⁸O₂, CH₃OH·S¹⁶O¹⁸O, CH₃OH·S¹⁸O¹⁶O, CH₃OD·SO₂, CD₃OH·SO₂, and CD₃OD·SO₂. The rotational spectra of the methanol·S¹⁶O¹⁸O and methanol·S¹⁸O¹⁶O complexes differ from the spectra of the other species. Due to the nonequivalent positions of the two oxygen atoms in the complex, no inversion splitting was observed in these species. Some of the transitions of the deuterium isotopomers were broader than usual because of the unresolved deuterium quadrupole splittings, and center frequencies for such clusters were visually estimated and used in the fit. The transition frequencies for all the observed isotopic species are available as supplementary material¹⁷ and the derived rotational constants are listed in Table III.

To determine the dipole moment of the methanol·SO₂ complex, second-order Stark shifts were measured for several A-state transitions. The second-order Stark coefficients were obtained from least-squares fitting of $\Delta\nu$ vs ϵ^2 and are listed in Table IV. A least-squares fit of these observed coefficients gave dipole components of $\mu_a=1.781(2)$ D, $\mu_b=0.543(23)$ D, $\mu_c=0.554(22)$ D, and a total dipole moment of $\mu_T=1.94(3)$ D. The Stark effect splittings were essentially the same for either inversion component.

IV. DISCUSSION

A. Structure and dipole moment

The structure of the complex could be determined unambiguously, since the spectra for nine isotopic species were analyzed. The presence of three selection rules indicates that the methanol·SO₂ complex has no symmetry plane. One can also expect that the methanol·SO₂ complex has a stacked

FIG. 1. Definition of the structural parameters for methanol·SO₂.

structure. In this configuration, the relative geometry of the two monomers in the complex can be specified by one distance and five angles. As shown in Fig. 1, $R_{C.M.}$ is the distance between χ_S , the center of the mass (COM) of SO₂, and χ_M , the center of mass of methanol. θ_S is the SO₂ tilt angle of the C₂ axis of SO₂ with respect to $R_{C.M.}$ and θ_M defines the methanol tilt angle between $R_{C.M.}$ and χ_M -O of methanol. The wagging angles of the SO₂ and methanol are defined by the angles Ψ_S ($\angle O_A-S-\chi_S-\chi_M$) and Ψ_M ($\angle H_1-O-\chi_M-\chi_S$), respectively. Finally, the dihedral angle was defined as Φ ($\angle S-\chi_S-\chi_M-O$).

In order to determine the structure of the complex, Schwendeman's computer program STRFTQ (Ref. 18) was used to fit the moments of inertia of all the isotopic species. It was assumed that the monomer structures were unchanged in the complexes and the literature values of the monomer geometries were used.¹⁹ The six structural parameters were varied in the fitting of the twenty seven moments of inertia with the resultant values given in Table V. The deviation of the fit (ΔI_{rms}) was $0.395 \text{ amu } \text{\AA}^2$. Schematic diagrams of the structure viewed along the c axis and a axis are shown in Figs. 2(a) and 2(b), respectively. As can be seen in Fig. 2, the structure of the methanol·SO₂ complex has a stacked configuration. The SO bonds approximately eclipse the methanol framework bonds, and the methanol framework plane is nearly parallel to the SO₂ plane.

The distance between the methanol and SO₂ monomers can be compared to expectations from the van der Waals (vdW) radii of relevant atoms. The distance between the sulfur atom and the carbon atom is 3.46 \AA , which is very close

TABLE V. Structural parameters from least squares fits of the moments of inertia.

	Structure		
	CH ₃ OH·SO ₂ ^a	H ₂ O·SO ₂ ^b	(CH ₃) ₂ O·SO ₂ ^c
θ_S (deg) ($\angle \chi_M - \chi_S - S$) ^d	68.8(10)	69.7(10)	85.8(6)
θ_M (deg) ($\angle \chi_S - \chi_M - O$)	86.9(57)	66.3(14)	72.6(3)
Ψ_S (deg) ($\angle O_A - S - \chi_S - \chi_M$)	76.3(5)	90	90
Ψ_M (deg) ($\angle \chi_S - \chi_M - O - H_1$)	80.8(48)	90	90
Φ (deg) ($\angle S - \chi_S - \chi_M - O$)	46.2(23)	0	0
$R_{C.M.}$ (Å)	3.081(1)	2.962(5)	3.05(1)
R_{S-O} (Å)	2.85(2)	2.824(16)	2.87(3)
ΔI_{rms} (amu Å ²) ^e	0.39	0.15	0.15

^aLeast-squares fit of 27 moments of inertia from the nine isotopic species.

^bReference 3.

^cReference 4.

^dStructural parameters defined in Fig. 1. Signs of the dihedral angles are consistent with the definition in Ref. 29.

^e $\Delta I = I_{X,Y,Z}(\text{obs}) - I_{X,Y,Z}(\text{calc})$ for a given isotopic species.

to the sum of the van der Waals radii of sulfur and carbon (3.50 Å).²⁰ The closest separation between an oxygen of the SO₂ and a methyl hydrogen is 2.5 Å assuming that the methyl group conformation is unchanged from methanol. This distance is slightly smaller than the sum of the van der Waals radii of oxygen and hydrogen (2.7 Å).²⁰ This configuration is consistent with a dipole–dipole interaction that tends to align

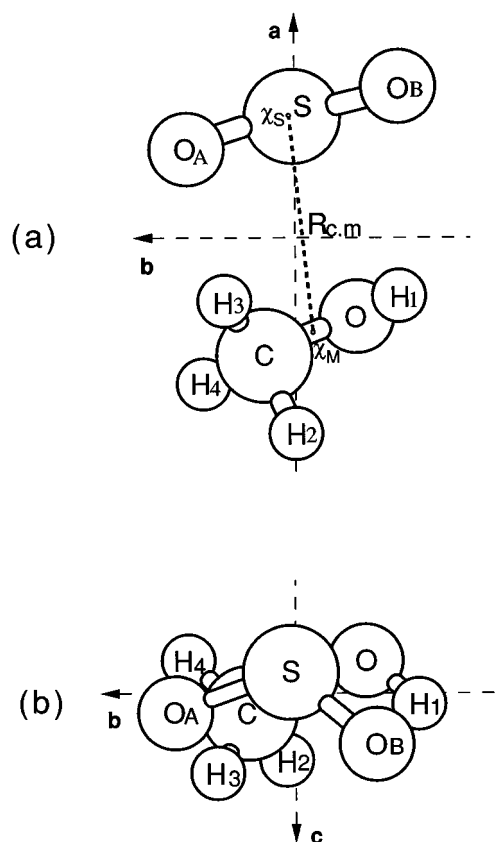


FIG. 2. Schematic diagram of the structure of the methanol·SO₂ complex in the principal axis system. (a) Viewed along the *c* axis; (b) viewed along the *a* axis. χ_M and χ_S are the centers of mass (COM) of the methanol and SO₂ monomer, respectively. $R_{C.M.}$ is the distance between the two COMs.

the dipole moments of the two monomers antiparallel. It may be possible that there is a interaction between the oxygen atom of SO₂ near the methyl group and a methyl hydrogen, since one S–O bond is directed to the methyl group. This also could make a positive contribution to the van der Waals interaction.

The structure parallels the symmetric stacked structures for H₂O·SO₂ and (CH₃)₂O·SO₂. The separation between the centers of mass of the two monomers was determined to be 3.081 Å, slightly larger than the 2.96 and 3.05 Å COM distances for the H₂O·SO₂ and DME·SO₂ complexes, respectively. However, these values are not strictly comparable since χ_M lies nearly on the C–O bond in methanol, unlike H₂O and (CH₃)₂O, where it lies along the C₂ axis. The comparison of the other structural parameters of methanol·SO₂ with that of the water·SO₂ and dimethyl ether·SO₂ complexes is shown in Table V. The intermolecular sulfur–oxygen distances are also listed in Table V. The sulfur–oxygen distance (S–O) in CH₃OH·SO₂ is slightly larger than that in H₂O·SO₂, and smaller than in (CH₃)₂O·SO₂. These results suggest that the van der Waals interaction may be the strongest in H₂O·SO₂.

As a check on the structural determination, Kraitchman's equations¹⁴ were used to determine the positions of the isotopically substituted atoms in the complex. The results are listed in Table VI. Using these coordinates, the C–O and O–H bond lengths in methanol and the O–O distance in SO₂ were calculated as 1.431, 1.154, and 2.470 Å, respectively. These are in good agreement with the C–O bond length in methanol of 1.425 Å and the O–O distance in SO₂ of 2.476 Å. The O–H bond length, however, differs appreciably from the value in the bare methanol monomer (~1 Å). A similar discrepancy in the O–H bond length in the methanol·Ar complex was observed by Tan *et al.*⁸ This variance is likely a result of the large amplitude “swinging” motion of the hydroxyl group in the complex which is markedly affected by deuteration.

The small uncertainties in the structural parameters listed in Table V are the statistical values from the fitting process. However, this is a vibrationally averaged structure which does not take into account how the large amplitude vibrational and tunneling motions in this weakly bound complex affect the moments of inertia. These effects, which vary with isotopic substitution, could be sizable. Consequently, we conservatively recommend that $R_{C.M.}$ and the angles should be within 0.05 Å and 5° of the equilibrium values.

Based on the structure of the methanol·SO₂ complex, the dipole moment components were estimated from the vector sum of the dipole moments of SO₂ and methanol. Due to the nearly antiparallel alignment of the monomer dipole moments, this gave $\mu_a = 0.23$ D, $\mu_b = 0.20$ D, and $\mu_c = 0.072$ D. Compared to the measured dipole moments (Table IV), all dipole moment components show a substantial difference between the estimated and measured values. The overall increase in the total dipole moment of the complex (1.6 D) is attributed to induction effects and can be compared to the increases in (CH₃)₂O·SO₂ and H₂O·SO₂ of 1.4 and 0.75 D, respectively. These are appreciable effects but still smaller

TABLE VI. The Cartesian coordinates of the atom positions in the principal axis system of methanol·SO₂ (Å). Coordinates listed under “Kraitchman” were determined using Kraitchman’s equations. Coordinates listed under “STRFTQ” were determined using the computer program STRFTQ which fitted the 27 moments of inertia.

	Kraitchman			STRFTQ		
	a	b	c	a	b	c
H ₁	1.315	1.508	0.298	-1.434	-1.360	0.270
O	1.634	0.631	0.381	-1.733	-0.728	-0.365
C	2.440	0.323	0.317	-2.375	0.339	0.326
H ₂				-3.246	-0.005	0.892
H ₃				-1.693	0.851	1.012
H ₄				-2.711	1.055	-0.430
O _A	0.689	1.325	0.155	0.616	1.323	0.165
O _B	1.345	1.026	0.535	1.452	-0.975	0.551
S				1.010	0.046	-0.353

than in amine·SO₂ complexes where increases of 2.7–3.0 D were observed.

B. Electrostatic modeling

Previous studies of complexes such as ethylene·SO₂ (Ref. 21), propene·SO₂ (Ref. 22), furan·SO₂ (Ref. 23), and benzene·SO₂ (Ref. 24) have shown that the Buckingham and Fowler (Ref. 25) electrostatic interaction model can rationalize conformational features of many vdW complexes. We therefore applied this model to our current system to explore its ability to rationalize the structure of the methanol·SO₂ complex.

In the Buckingham–Fowler model, the charge distribution of each monomer is described by sets of point multipoles, which are located on the atoms and sometimes at bond midpoints, and the electrostatic interaction energy is calculated between the multipole moments. A hard sphere (van der Waals radii) interaction is used as a repulsive term. The distributed multipole values for SO₂ were taken from Ref. 25. Those for methanol were determined by an *ab initio* calculation using the CADPAC program with a 6-31G** basis set.²⁶ (Values up to quadrupole moments were used and are provided in the supplementary materials.) The electrostatic interaction energy between the two monomers as a function of torsional angle Φ was calculated while all the other parameters were fixed at the values in Table V. The energy versus Φ calculation gave a minimum (−3.3 kcal/mol) at 36.2° near the experimental value of 46.2°. The electrostatic energy as a function of the tilt angles of SO₂ (θ_S) and methanol (θ_M) with the other structural parameters fixed was also calculated. The calculated and observed minima values for the SO₂ tilt angle are 68.8° and 77.5°, respectively. On the other hand, a similar calculation for the tilt angles of methanol did not give a minimum. Of course, this model does not include the dispersion and induction interactions, nor a realistic treatment of repulsions. Nevertheless, it would appear that the anisotropy in the electrostatic interaction terms leads to reasonable qualitative predictions of the orientation of SO₂ relative to a fixed methanol substrate. This parallels the results for a number of SO₂ complexes recently studied by us [SO₂

dimer (Ref. 27) and acetylene·SO₂ (Ref. 22) are noteworthy exceptions].

C. Large amplitude motions

1. The inversion motion

As mentioned in Sec. III each rotational transition in methanol·SO₂ is split by an inversion motion into two components. The magnitude of the inversion splitting varies for different dipole selection rules. The typical values are 1, 30, and 6 MHz for the *a*-, *b*-, and *c*-type transitions, respectively (in the normal species). Due to the low temperature of the supersonic expansion, we need to consider only the lowest two inversion levels, designated as + and −, respectively. The aforementioned dipole selection rule dependence of the inversion splitting suggests that the *a* and the *c* dipoles connect inversion levels with the same parity while the *b* dipole connects inversion levels with the opposite parity (these results can be verified by a direct fit of the inversion splitting, *vide infra*). These dipole selection rules are depicted in Fig. 3. Because the *b*-dipole transitions connect inversion levels with opposite parity, the direction of the *b*-dipole moment is reversed by the inversion motion. The dipole selection rules were not strictly followed for the *E*-state transitions due to wavefunction mixing caused by torsion-rotation coupling. Hence quartet structures were observed for some *E* lines, as also shown in Fig. 3. The inversion splitting also has a strong isotopic dependence. It is much smaller in the isotopomers with the hydroxyl hydrogen deuterated and it is completely quenched in the isotopomers involving the singly substituted S¹⁶O¹⁸O. Based on the geometry of the complex, the inversion motion should occur between the configuration shown in Fig. 2(a) [also shown in Fig. 4(a)] and one of the equivalent configurations arrived by the symmetry operations (AB) or (AB)(23)*, where the symmetry operations are those defined by Longuet–Higgins²⁸ for the molecular symmetry group. The configuration obtained by the symmetry operation (AB), i.e., an exchange of the two oxygen atoms in SO₂, can be readily ruled out because this operation will not alter the direction of the *b*-dipole moment of the complex. Therefore the inversion occurs between the two configurations shown in Figs. 4(a) and 4(b). [Figure 4(b)

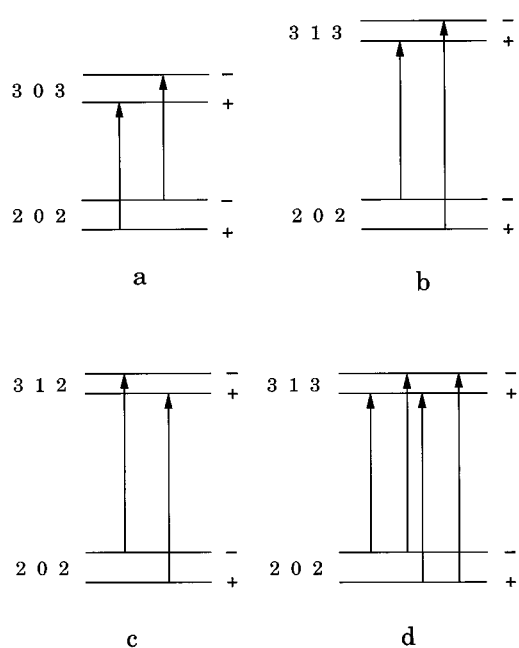


FIG. 3. Transition diagrams showing dipole selection rules of the rotation-inversion transitions of methanol·SO₂. (a) *a*-type transitions; (b) *b*-type transitions; (c) *c*-type transitions; and (d) *E*-state transitions, which do not follow any of the above.

is obtained by applying the symmetry operation (AB)(23)* to Fig. 4(a).] One can visually verify that the *b* dipole is reversed between the two configurations while the *a* and the *c* dipoles remain unchanged.

The “rotation free” or “pure” inversion splitting of each isotopomer of the complex can be obtained by a fit to the *A*-state rotation-inversion transitions. In such fits we assume that each inversion state has its own effective rotational and distortion constants and its own origin (in much the same way as treating the two inversion states as two vibrational states). The separation between the two “origins” (Δ_{inv}) then gives the “pure” inversion splitting, which is simply the

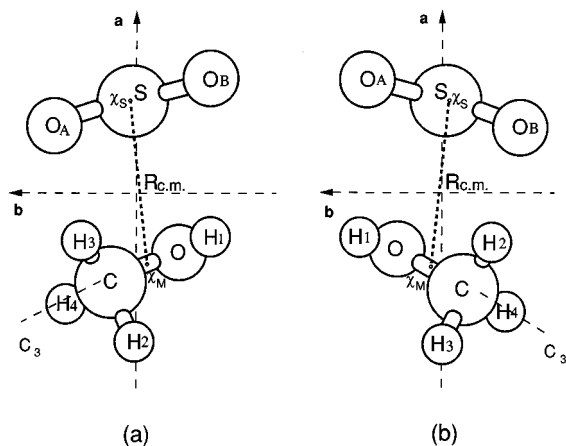


FIG. 4. Configuration (a) is energetically equivalent to configuration (b). Tunneling between (a) and (b) configurations results in the “inversion” splitting observed in the rotational spectrum of methanol·SO₂.

splitting caused by tunneling between the two equivalent configurations of the complex shown in Figs. 4(a) and 4(b). The so-called “combination sum rule” check⁵ was used in the initial assignments, and appropriate dipole selection rules were assumed (and verified). The standard deviations of the fits were typically about 20 kHz, similar to those obtained in the fit of the averaged frequencies. The resultant “pure” inversion splittings (Δ_{inv}) for all the isotopomers studied are listed in Table III.

In the study of methylacetylene·SO₂, the “rotation free” inversion splittings were used to estimate a barrier to inversion using a simple one-dimensional rotor Hamiltonian. Such an approach is not attempted here since the inversion pathway could not be easily identified. We can only speculate that the inversion is probably some kind of wagging motion, involving both the SO₂ and the methanol subunits. From the splittings listed in Table III one may get some idea as to how much involvement each atom has in the inversion motion.

The unusual linear term required to fit the *A*-state transitions of the complex can be shown to be related to the inversion. The coefficient of this term (D_a) for various isotopomers of the complex is listed in Table III. One can see that it is approximately proportional to the corresponding inversion splitting and becomes zero when the inversion motion is reduced or quenched by deuteration of the hydroxyl group or by breaking the SO₂ symmetry isotopically. The origin of this linear term (which resembles a first-order Coriolis term) is still not entirely clear, but we speculate that rotation-inversion or torsion-inversion coupling may play a role here. Moreover, an exchange of the two oxygen atoms in SO₂, if feasible, may produce a shift in the rotational energy which can also introduce some unexpected terms in the rotational Hamiltonian.

2. The methyl group internal rotation

Since the methyl group in methanol undergoes internal rotation (torsion), each rotation-inversion transition of methanol·SO₂ is further split into an *A* and *E* component. It is possible to estimate the height of the potential barrier hindering the internal rotation from the observed *A*-*E* splitting (or a simultaneous fit to the *A* and *E* lines) using well-established formalisms. The torsional barriers obtained for methanol·SO₂ and its isotopomers are listed in Table III. The torsional analysis can be shown to be consistent with the structural analysis by comparison of the direction cosines of the methyl group symmetry axis obtained using the two methods. The direction cosines determined in the torsional analysis are listed in Table III. To calculate the direction cosines from the structural parameters, the Kraitchman coordinates of the carbon and oxygen atoms in methanol were used first to obtain the direction of the O–C bond. Then, taking into account that the methyl symmetry axis is tilted about 3° from the O–C bond, we obtain the direction cosines for the methyl group symmetry axis as $\lambda_a=0.559$, $\lambda_b=0.701$, and $\lambda_c=0.443$. These numbers agree quite well with the corresponding ones listed in Table III.

As can also be seen in Table III, V_3 varies for different isotopomers, especially for the deuterated species. These observed barriers, however, are all substantially smaller than in

TABLE VII. Comparison of the measured and calculated apparent torsional barrier heights of various isotopomers of methanol·SO₂. See Ref. 8 for details of the calculations. $W_1 = 2\langle E|p_\alpha|E\rangle$. The observed values were obtained from spectral analyses and the calculated values were obtained from diagonalization of Eq. (3). $\nu_1 = 535 \text{ cm}^{-1}$ for all isotopomers.

	W_1 (Calc)	V_3 (cm ⁻¹) (Obs)	V_3 (cm ⁻¹) (Calc)
CH ₃ OH·SO ₂	0.1334	128.67	128.67
CH ₃ OD·SO ₂	0.0626	164.80	169.87
CD ₃ OH·SO ₂	0.0283	107.19	108.76
CD ₃ OD·SO ₂	0.0113	139.11	139.02

bare methanol, for which $V_3 \approx 373 \text{ cm}^{-1}$. This large decrease in the methyl torsional barrier height has also been observed in other methanol complexes. Recent studies^{8,9} have shown that such a “barrier reduction effect” is only apparent, caused by the lightness of the hydroxyl hydrogen which can undergo large amplitude “librational” motions. Fraser *et al.*⁹ proposed the following torsional Hamiltonian to account for this barrier reduction effect

$$H = Fp_\alpha^2 + F_1p_\theta^2 - 2F_1p_\alpha p_\theta + V_3(1 - \cos 3\alpha)/2 + v_1(1 - \cos \theta)/2, \quad (3)$$

where H is the Hamiltonian describing the large amplitude internal rotations of the methyl group and the hydroxyl group around the a axis of methanol. α is the methyl group internal rotation angle with respect to the O–H bond, θ is the internal rotation angle of the OH group. p_α and p_θ are the conjugate momenta of α and θ , respectively. $F_1 = \hbar^2/2I_1$ where I_1 is the moment of inertia of the OH top about the a axis of methanol. $F = \hbar^2/2I_r$ where $I_r = I_1I_\alpha/(I_1 + I_\alpha)$ and I_α is the moment of inertia of the methyl group around its symmetry axis. V_3 is the actual methyl group torsional barrier height, and may be approximated by the value in bare methanol. v_1 is the first term in a Fourier expansion of the potential function describing the librational motion. If the remaining terms fall off fast, it is approximately equal to the height of the barrier hindering the OH wagging motion.

Equation (3) can be linked to the overall rotational motion via the expectation value $W_1 = 2\langle E|p_\alpha|E\rangle$, which is directly proportional to the first order Coriolis coupling (for the E state, not to be confused with the D_aP_a term) in the rotational spectra. If one knows v_1 , Eq. (3) can be used to calculate $|E\rangle$ and subsequently W_1 . W_1 can then be used to obtain the apparent methyl group torsional barrier height. Unfortunately, v_1 is usually not known due to the lack of vibrational information for these methanol complexes. Therefore, Eq. (3) is often used in reverse to determine v_1 , using the experimentally determined apparent V_3 . For the normal species methanol·SO₂, v_1 is calculated to be 535 cm^{-1} .

It can be argued that using a simple one term cosine function for the wagging potential in the present problem may not be a very good approximation. Moreover, using the monomer value of V_3 in Eq. (3) is questionable since it is known that SO₂ may have some effect on the methyl torsional barrier height upon complexation.⁵ Thus the value of

v_1 obtained has to be regarded as very approximate. It is therefore quite gratifying that with this v_1 and Eq. (3) one can predict the apparent barrier heights of the other isotopomers of methanol·SO₂ very well. These results are reported in Table VII from which it can be seen that the largest error between the observed and predicted V_3 values is only about 3%. This seems to indicate that the simple model proposed by Fraser *et al.* accounts well for the dynamical aspect of the barrier reduction effect, and suggests that the methyl group barrier is not markedly affected by complexation.

V. CONCLUSION

The microwave spectra of methanol·SO₂ and eight of its isotopomers were assigned. Spectral analysis gave rotational constants of these species which led to the determination of the structure of the complex. The complex was found to have a stacked structure, with a centers-of-mass distance of $3.08(5) \text{ \AA}$ between the two monomers. The dipole moment of methanol·SO₂ was determined from Stark effect splittings. A large a -dipole moment was observed indicating sizeable induction effects. The projection of the dipole moments of the two monomers on the b - c plane are aligned close to antiparallel indicating electrostatic effects are a significant factor in determining the structure. Electrostatic calculations using a distributed multipole moment model also provided some support for the importance of electrostatic interactions. Spectral splitting associated with both the internal rotation of the methyl group and an inversion motion was observed. Analysis of the internal rotation of the methyl group was carried out, giving an effective methyl barrier of 129 cm^{-1} . It was shown that this barrier reduction is only apparent and associated with the neglect of the large amplitude librational motion of the light hydroxyl hydrogen.

ACKNOWLEDGMENTS

This work was supported by the National Science Foundation, Washington, D.C. The authors are grateful to the donors of the Petroleum Research Fund, administered by the American Chemical Society, for the support of this work. We are grateful for an allotment of computing time at the San Diego Supercomputing Center and appreciate some helpful advice from Susan Forest on the preparation of the manuscript.

- J. J. Oh, M. S. LaBarge, J. Matos, J. W. Kampf, K. W. Hillig II, and R. L. Kuczkowski, *J. Am. Chem. Soc.* **113**, 4732 (1991).
- J. J. Oh, K. W. Hillig II, and R. L. Kuczkowski, *J. Am. Chem. Soc.* **95**, 7211 (1991).
- K. Matsumura, F. J. Lovas, and R. D. Suenram, *J. Chem. Phys.* **91**, 5887 (1989).
- J. J. Oh, K. W. Hillig II, and R. L. Kuczkowski, *J. Am. Chem. Soc.* **30**, 4583 (1991).
- X.-Q. Tan, L.-W. Xu, M. J. Tubergen, and R. L. Kuczkowski, *J. Chem. Phys.* **101**, 6512 (1994).
- F. J. Lovas, R. D. Suenram, G. T. Fraser, C. W. Gillies, and J. Zozom, *J. Chem. Phys.* **88**, 722 (1988).
- F. J. Lovas, S. P. Belov, M. Yu. Tretyakov, J. Ortigoso, and R. D. Suenram, *J. Mol. Spectrosc.* **167**, 191 (1994).
- X.-Q. Tan, L. H. Sun, and R. L. Kuczkowski, *J. Mol. Spectrosc.* **171**, 248 (1995).
- G. T. Fraser, F. J. Lovas, and R. D. Suenram, *J. Mol. Spectrosc.* **167**, 231 (1994).

- ¹⁰T. J. Balle and W. H. Flygare, *Rev. Sci. Instrum.* **52**, 33 (1981).
- ¹¹R. K. Bohn, K. W. Hillig II, and R. L. Kuczkowski, *J. Phys. Chem.* **93**, 3456 (1989).
- ¹²K. Tanaka, H. Ito, K. Harada, and T. Tanaka, *J. Chem. Phys.* **80**, 5893 (1984).
- ¹³R. L. Kuczkowski and A. Taleb-Bendiab, in *Structures and Conformations of Non-Rigid Molecules*, edited by J. Lanne, M. Dakkouri, B. van der Veken, and H. Oberhammer (Kluwer, Dordrecht, 1993), pp. 257–276.
- ¹⁴W. Gordy and R. L. Cook, *Microwave Molecular Spectra*, 3rd. Ed. (Wiley-Interscience, New York, 1984).
- ¹⁵A. Taleb-Bendiab, K. W. Hillig II, and R. L. Kuczkowski, *J. Chem. Phys.* **98**, 3627 (1993).
- ¹⁶F. Rohart, *J. Mol. Spectrosc.* **57**, 301 (1975).
- ¹⁷See AIP document no. PAPS JCPA-103-6440-26 for 26 pages of tables. Order by PAPS number and journal reference from American Institute of Physics, Physics Auxiliary Publication Service, Carolyn Gehlbach, 500 Sunnyside Boulevard, Woodbury, New York 11797-2999, Fax: 516-576-2223, e-mail: janis@aip.org. The price is \$1.50 for each microfiche (98 pages) or \$5.00 for photocopies of up to 30 pages, and \$0.15 for each additional page over 30 pages. Airmail additional. Make checks payable to the American Institute of Physics.
- ¹⁸R. H. Schwendeman, in *Critical Evaluation of Chemical and Physical Structural Information*, edited by D. R. Lide and M. A. Paul (National Academy of Sciences, Washington, D.C., 1974), pp. 94–115.
- ¹⁹M. C. L. Gerry, R. M. Lees, and G. Winnewisser, *J. Mol. Spectrosc.* **61**, 231 (1976); S. Saito, *ibid.* **30**, 1 (1969).
- ²⁰A. Bondi, *J. Phys. Chem.* **68**, 441 (1964).
- ²¹A. M. Andrews, A. Taleb-Bendiab, M. S. LaBarge, K. W. Hillig II, and R. L. Kuczkowski, *J. Chem. Phys.* **93**, 7030 (1990).
- ²²A. M. Andrews, K. W. Hillig II, R. L. Kuczkowski, A. C. Legon, and N. Howard, *J. Chem. Phys.* **94**, 6947 (1991).
- ²³J. J. Oh, L.-W. Xu, A. Taleb-Bendiab, K. W. Hillig II, and R. L. Kuczkowski, *J. Mol. Spectrosc.* **153**, 497 (1992).
- ²⁴A. Taleb-Bendiab, K. W. Hillig II, and R. L. Kuczkowski, *J. Chem. Phys.* **97**, 2996 (1992).
- ²⁵A. D. Buckingham and P. W. Fowler, *Can. J. Chem.* **63**, 2018 (1985).
- ²⁶R. D. Amos and J. E. Rice, *The Cambridge Analytic Derivatives Package, Issue 4.0* (Cambridge, England, 1987).
- ²⁷A. Taleb-Bendiab, K. W. Hillig II, and R. L. Kuczkowski, *J. Chem. Phys.* **94**, 6956 (1991).
- ²⁸H. C. Longuet-Higgins, *Mol. Phys.* **6**, 445 (1963).
- ²⁹E. B. Wilson, Jr., J. C. Decius, and P. C. Cross, *Molecular Vibrations* (McGraw Hill, New York, 1955).